Photoelastic study of the foundation elasticity effect on the stresses in a gravity dam

K. CHANDRASHEKHARA AND MOHAMMAD TAFSEERUDDIN
Department of Civil Engineering, Indian Institute of Science, Bangalore 560 012.

Abstract

Stress distribution in gravity dams supported on foundation having same elastic modulus (homogeneous case) as well as having different elastic modulii (composite case) compared to the dam material has been obtained using two-dimensional photoelastic analysis. The photoelastic composite model is prepared using two different materials having different modulus of elasticity at elevated temperature (110° C). Stress distributions in the dam with and without opening have been obtained for hydrostatic loading only and are compared with some available solutions.

Key words : Photoelasticity, composite body, gravity dam, stress analysis.

1. Introduction

Stress distribution in gravity dams founded on rock having elastic modulus different from that of dam material is of practical interest. It is known that the vertical stress distribution will not be linear as indicated by simple stress analysis[1] and the stress distribution in general will be nonlinear at the junction of the dam and rock foundation (interface) as well as in the bottom portion of the dam. Several attempts have been made by earlier investigators[2,3], using either theoretical or experimental approach, to take into account the foundation elasticity effect in the stress analysis of the dam. However, these approaches were rather complicated and did not give any definite ideal to the designer. Recently this problem has been successfully tackled by Zienkiewicz et al[4] and Varshney[5,6] using finite element method. Very little information is available on the experimental analysis of this problem. However, Varshney[6] has made an attempt to get some idea of stress distribution in the dam using photoelastic method. In the experiment, to achieve different ratios of modulus of elasticity between dam and foundation, he reduces the thickness either of the dam or foundation. This type of model when used in photoelastic stress analysis can give distorted stress distribution particularly along the interface. In fact the reason for the unsuccessful application of the

187

photoelastic method to this type of problem is due to the nonavailability of photo-elastic materials having a very wide range of elastic constants—particularly the modulus of elasticity at room or elevated temperature. However, the situation has improved now with the development of techniques to obtain materials having different elastic modulus at room or elevated temperature by using different types of epxoy resins and hardeners[7].

·Apart from this, the photoelastic method gives at a point the difference of principal stress and shear stress and with this data alone it is not possible to obtain all the components of stress in a two-dimensional model. Normally the photoelastic method is supplemented by some numerical method and one of the widely used numerical method is the shear difference method[8]. It is known that this method can give large errors in the stresses determined due to cumulative nature of the error in the integration procedure. Recently, Chandrashekahara et al.[9,10] have suggested methods to determine the interior stresses from the known or determined boundary stresses as well as the interface stresses in a composite body directly from the photoelastic data.

In this paper, the stress distribution in a gravity dam founded on a rock foundation having modulus of elasticity different from that of dam material and subjected only to hydrostatic load using photoelastic method has been presented. The stress distribution in the dam with and without openings has been studied in detail and the results have been compared with those obtained for a dam founded on a rock foundation having the same modulus of elasticity of the dam material in order to bring out clearly the foundation elasticity effect on the stresses. For the determination of interior and inter-face stresses the methods developed by Chandrashekhara et al.[9,10], have been used. It is believed that following this and by making use of materials having different modulus of elasticity already developed , a detailed parametric study of the foundation elasticity effect on the stresses in a gravity dam could be made.

2. Model preparation

2.1. Homogeneous model

This case corresponds to a dam founded on a rock foundation having the same modulus of elasticity as the dam material. A photoelastic model representing the dam and foundation was prepared using epoxy resin Araldite CY 230 (supplied by M/s Ciba and Co., Bombay). The casting of the model was carried out in a specially prepared plexiglas mould. The following composition of resin and hardener was used for the casting.

> Araldite CY 230—100 parts by weight.
> Hardener HN 951—10 parts by weight.

Since the reaction between Araldite and the hardener is exothermic, in order to reduce large temperature rise of the mixture, Araldite CY 230 was initially cooled to

10° C and the {hardener was mixed with this precooled Araldite. To ensure proper mixing, the mixture was thoroughly stirred using a mechanical stirrer, then filtered through glass wool to remove all the entrapped air and was poured into the mould. The material was allowed to set at room temperature and the model was stripped off from the mould after 24 hours. The model was then finished to the correct dimensions and stored in a desicator to protect it from time edge effect.

For preparing a model with an opening, the following procedure was adopted. A plexiglas piece having the exact dimensions of the hole was first cut out. It was then placed at the corresponding position of the opening in the mould. The casting was carried out in an identical way as described earlier. After stripping off the model from the mould, the plexiglas piece also was removed leaving the required shape and dimensions of the opening in the model.

2.2. Composite model

The photoelastic composite model was prepared using two different birefringent materials, namely, Columbia Resin (CR-39) and Araldite CY 230. CR-39 which is available in sheet form was used to represent the foundation of the dam. A mould was prepared in plexiglas with a provision to accommodate a piece of CR-39, representing the foundation, in correct position. The composition of Araldite and hardener used for casting the Araldite portion of the model as well as the casting procedure was same as explained earlier. Special precautions were taken to avoid shrinkage stresses along the interface. The dimensions of the model, and of the opening, the position of the opening, etc., are given in Table I (Fig. 1). Altogether, stress distribution in eight models—four homogeneous and four composite models with and without openings—was obtained.

Table I

Model dimensions

| Sl. No.	Height of dam in cm (h)	Width of dam in cm (b)	Position of opening (h_2)	Opening dimensions		
				Width in cm (b_1)	Height in cm (h_1)	Remarks
1.	11·0	10·5	..	..	..	HM*
2.	11·0	11·45	..	..	..	CM
3.	11·0	11·5	At the junction of dam and foundation	0·6	0·7	HM
4.	10·8	10·2	—do—	0·6	0·7	CM
5.	10·5	10·2	1·9 cm from interface	0·6	0·7	HM
6.	10·6	10·2	—do—	0·6	0·7	CM
7.	11·5	11·0	8·4 cm from interface	0·6	0·7	HM
8.	11·1	10·2	—do—	0·6	0·7	CM

*HM—Homogeneous Model; CM—Composite Model.
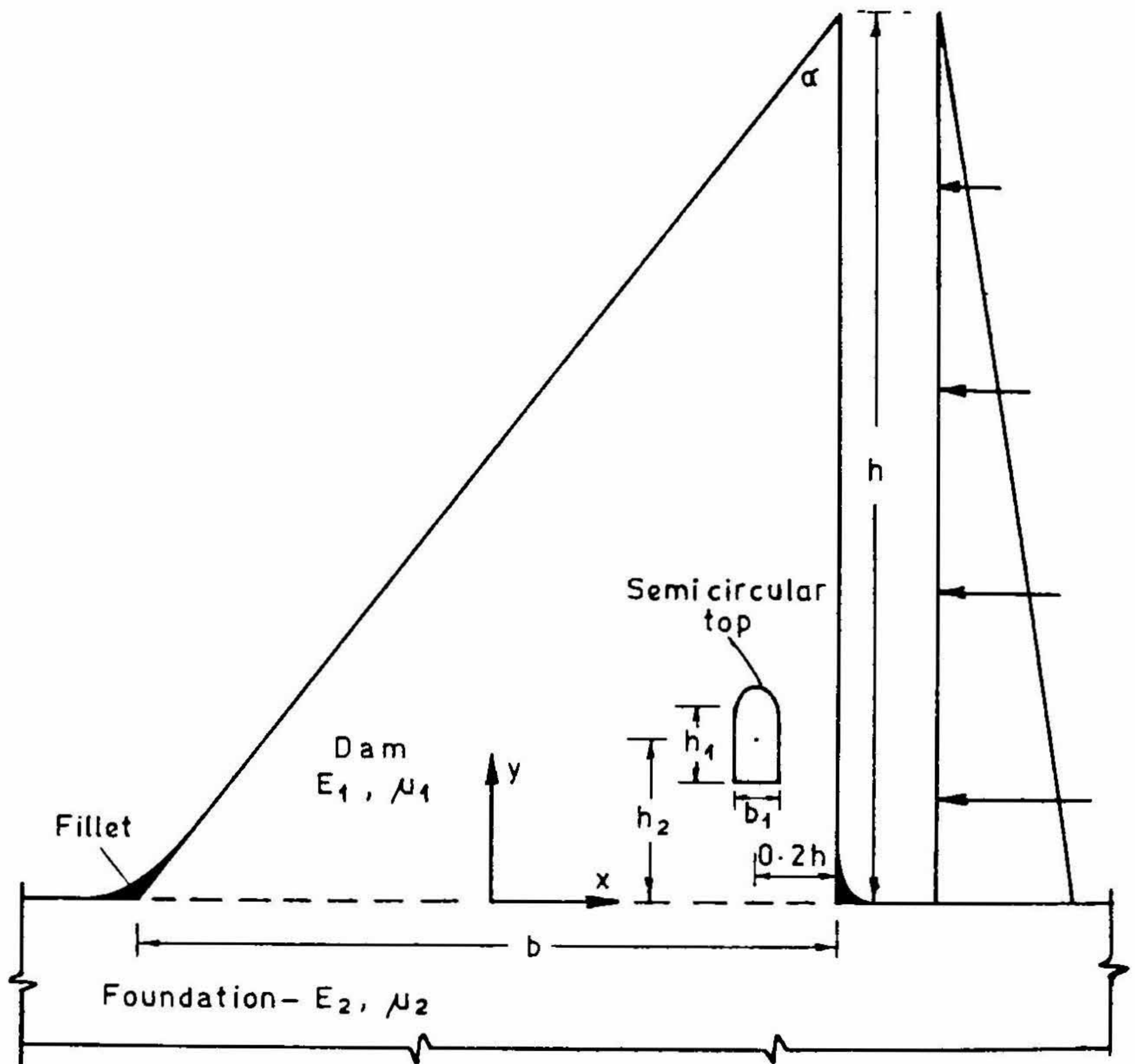
Fig. 1.

3. Loading arrangement

The hydrostatic loading (water load) was simulated by using a mechanical loading system. In this the hydrostatic loading which is a triangular type of loading, was achieved by dividing the triangle into 4 divisions as shown in Fig. 1. The centre of gravities of each of the trapezium and triangle was found out and a concentrated load at this point was applied through a base plate. In order to prevent concentration of the loading, etc., a thin packing of cardboard was given between the load base plate and the model. The procedure gave a satisfactory representation of the hydrostatic loading.

3.1 *Photoelastic method*

Araldite CY 230 and CR–39, the two materials used for manufacturing composite models, had almost the same modulus of elasticity at room temperature; while at a higher temperature it was different. Hence a stress freezing method was adopted in the stress analysis. Essentially the method consists of (i) applying the load on the model and then heating the model slowly (at about 2° C/hour) in an oven to a temperature called the critical temperature (110° C), (ii) soaking the model at this temperature (110° C) for about two hours, (iii) cooling slowly (at 1° C/hour) to room temperature, (iv) unloading and then observing the isochromatic pattern in a polariscope.

From the isochromatic pattern one can determine the difference of principal stress at a point by making use of the stress-optic law which can be written as

$$\sigma_1 - \sigma_2 = \frac{N f_\sigma}{t} \qquad (1)$$

where

σ_1 and σ_2 are the principal stresses

N—isochromatic fringe order at a point

f_σ —material fringe value

t—thickness of the model.

Along a free boundary, the isochromatic pattern directly gives the principal stress. It is also possible to determine the cartesian shear stress at a point from the isochromatic and isoclinic patterns as

$$\tau_{xy} = \left(\frac{\sigma_1 - \sigma_2}{2}\right) \sin 2\theta \qquad (2)$$

where θ is the isoclinic parameter.

3.2. *Cailbration of material*

For determining the difference of principal stress at point in the model using eqn. (1), it is necessary to know, in terms of stress, the material fringe value (f_σ), of the material. A circular disc subjected to two diametrically opposite concentrated load was chosen for determining the material fringe value. The material fringe value was determined both for Araldite CY 230 and CR–39 at room and critical temperatures (110° C) and the values are given in Table II.

Since the composite model had two different materials, their modulus of elasticity and Poisson's ratio were determined at room and critical temperatures. For this, a beam specimen, made out of the materials, subjected to pure bending was made use of.

By measuring the deflection of the beam accurately, the modulus of elasticity was computed using the well known beam deflection equations. This was cross-checked by determining the modulus of elasticity using disc and ring specimens[11]. In this method, in addition to modulus of elasticity, the Poisson's ratio also could be determined. It was found that the Poisson's ratio for the two materials at room temperature and at elevated temperature (100° C) was around 0·36 and 0·45, respectively.

It may be observed from Table II that the ratio of modulus of elasticity of CR–39 —Araldite is 1·45 at room temperature and 17 at elevated temperature (110° C).

4. Determination of stresses

For the complete determination of interior stresses, the method suggested by Chandra-shekhara et al[11] has been used. If on the other hand, the stress distribution is required only along a particular section, (for example, for homogeneous model along the junction of dam and foundation) another numerical method[12] which makes use of the photo-elastic data obtained along that section as well as at two other sections on either side of it has been suggested. These two methods are briefly described here.

4.1. Determination of interior stresses

The basic equations of two-dimensional elasticity are rewritten in the following form:

$$\nabla^2 S = 0 \tag{3}$$

$$\nabla^2 D = \frac{\partial^2 S}{\partial y^2} - \frac{\partial^2 S}{\partial x^2} \tag{4}$$

$$\nabla^2 \tau_{xy} = -\frac{\partial^2 S}{\partial x \partial y} \tag{5}$$

Table II

Property	Material			
	Araldite CY 230		CR–39	
	27° C	110° C	27° C	110° C
Modulus of elasticity in kg/sq. cm.	$1·36 \times 10^4$	$1·58 \times 10^2$	$1·91 \times 10^4$	$2·69 \times 10^3$
Material fringe value f_σ in kg/cm/fringe	13·05	0·366	15·0	3·83

where

$$\nabla^2 = \left(\frac{\partial^2}{\partial x^2} + \frac{\partial^2}{\partial y^2}\right) ; \quad S = (\sigma_1 + \sigma_2) = \sigma_x + \sigma_y$$

$$D = \sigma_x - \sigma_y.$$

Equations (3) to (5) are used to determine all the three stress components in the interior of the body. First eqn. (3) is solved. To do this the boundary values of sum of principal stresses should be known. This can be easily determined from the photoelastic experiment. Since the sum of the principal stresses is determined at discrete points along the boundary, it is advantageous to solve eqn. (3) (as well as eqns. (4) and (5) later) numerically by using the finite difference method. Equation (3) can be expanded in difference form about a point $O\,(i, j)$ (Fig. 2), for a square mesh, as

$$S_{i,j} = (S_{i+1,j} + S_{i-1,j} + S_{i,j+1} + S_{i,j-1})/4. \tag{6}$$

Similarly eqns. (4) and (5) can be expanded in finite difference form to give the recurrence equations for D for τ_{xy} respectively. They are

$$D_{i,j} = [(D_{i+1,j} + D_{i-1,j} + D_{i,j+1} + D_{i,j-1})$$
$$- (S_{i,j-1} + S_{i,j+1} - S_{i-1,j} - S_{i+1,j})/4 \tag{7}$$

$$(\tau_{xy})_{i,j} = [(\tau_{xy})_{i+1,j} + (\tau_{xc})_{i-1,j} + (\tau_{xy})_{i,j+1}$$
$$+ (\tau_{xy})_{i,j-1} - (S_{i+1,j+1} + S_{i-1,j-1} - S_{i+1,j-1}$$
$$- S_{i-1,j+1})]/4. \tag{8}$$

Solving the recurrence eqn. (6), sum of the principal stresses in the interior could be determined. After this, eqns. (7) and (8) are solved to determine the difference of
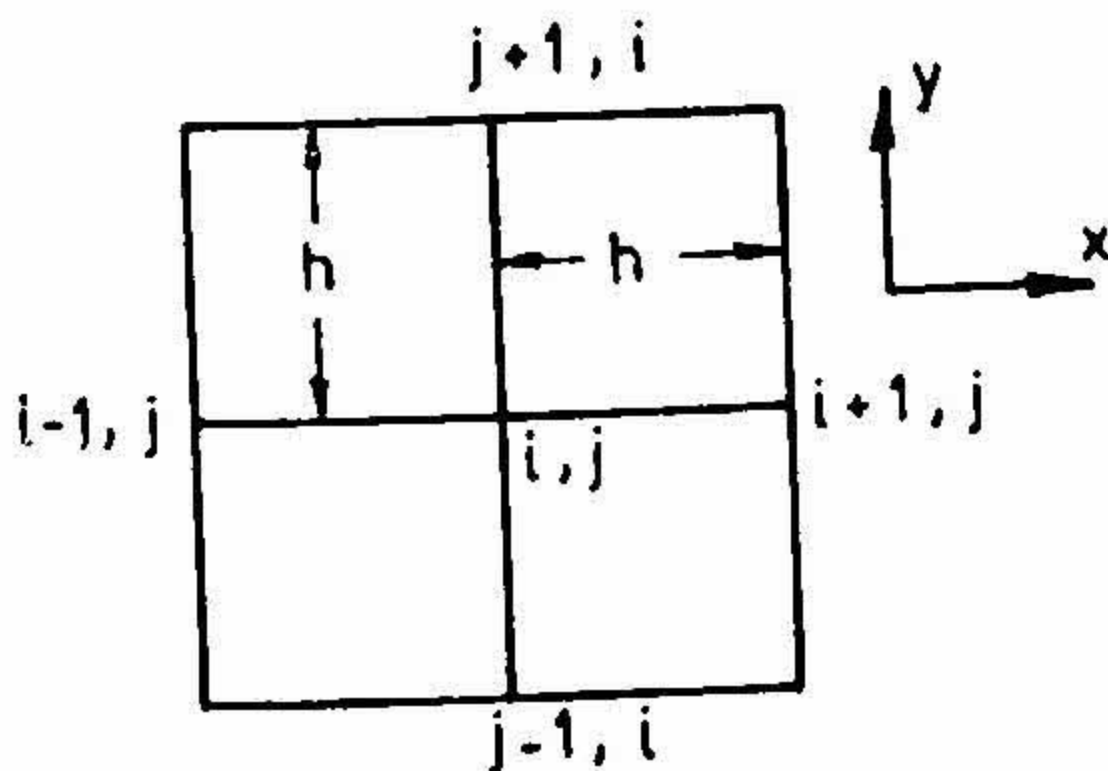

FIG. 2.

normal stresses (D) and shear stress (τ_{xy}). From the known sum and difference of normal stresses in the interior, the individual value of the normal stresses can be obtained.

If the stress distribution along a particular section is required the following numerical method can be used. From the photoelastic data, the difference of normal stresses can be obtained as

$$(\sigma_x - \sigma_y) = \frac{Nf_\sigma}{2} \cos 2\theta. \tag{9}$$

The values of difference of normal stresses can also be obtained using eqn. (9) along two sections $i - 1$ and $i + 1$ (Fig. 3). The equilibrium equations in two dimensions can be rewritten as

$$\frac{\partial^2 P}{\partial x^2} = -\frac{\partial^2 D}{\partial y^2} \tag{10}$$

$$\frac{\partial^2 \bar{Q}}{\partial y^2} = \frac{\partial^2 D}{\partial x^2} \tag{11}$$

where $\bar{P} = 2S + D; \ \bar{Q} = 2S - D.$

Equation (10) can be expanded in finite difference form as

$$(\bar{P}_{i-1,j} - 2\bar{P}_{i,j} + \bar{P}_{i+1,j})/h_1^2 = f_1(i, j) \tag{12}$$

where

$$f_1(i, j) = -(D_{i,j+1} - 2D_{i,j} + D_{i,j+1})/h^2$$

and h_1 and h are the grid spacing in x and y direction respectively.
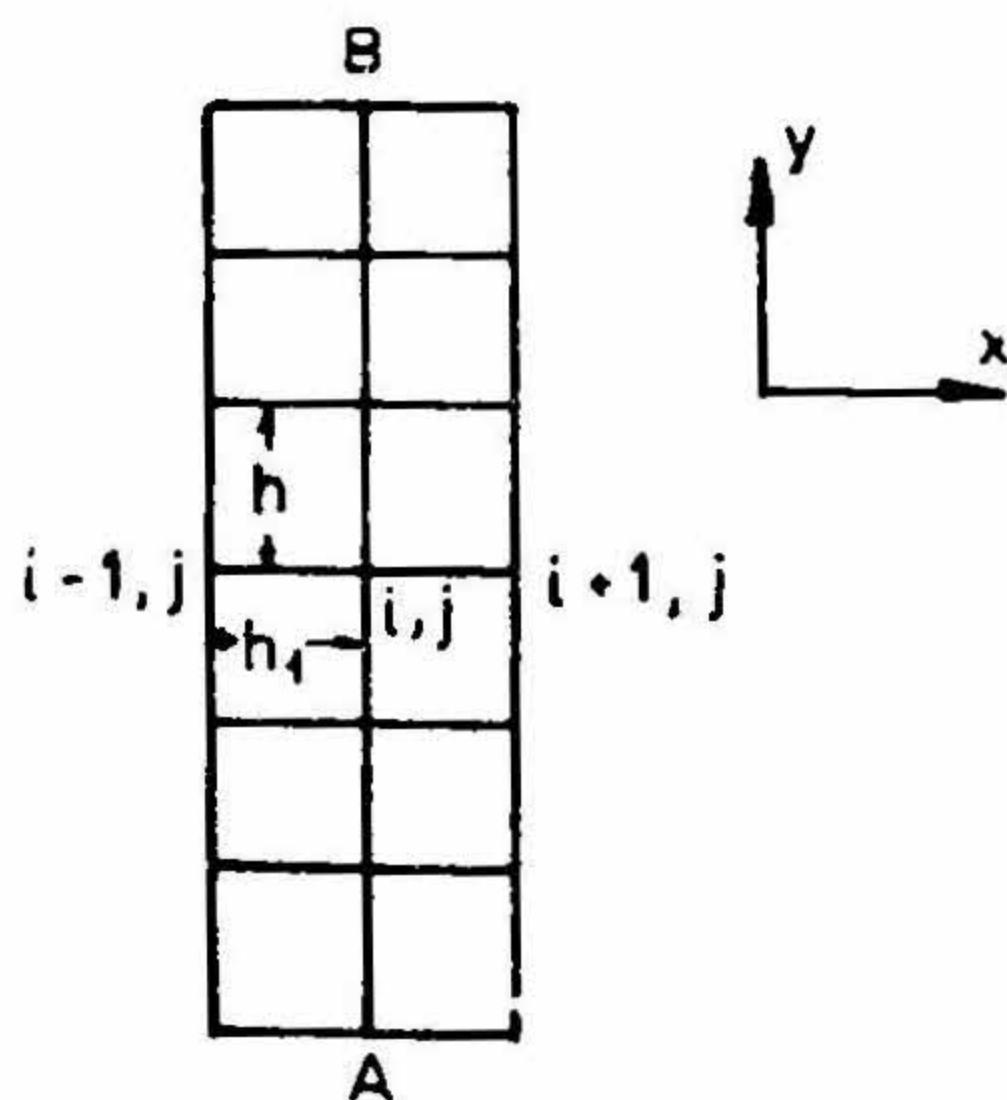
FIG. 3.

Similarly eqn. (11) can be expanded in finite difference form as

$$(\bar{Q}_{i,j-1} - 2\bar{Q}_{i,j} + \bar{Q}_{i+1,j})/h^2 = f_2(i,j) \tag{13}$$

where

$$f_2(i,j) = [D_{i+1,j} + D_{i-1,j} - 2D_{i,j}]/h_1^2.$$

Equation (12) is to be solved if the stresses along a section parallel to x-axis are required while eqn. (13) is to be solved if the stresses are required along a section parallel to y-axis. This method was used to determine the stresses along the junction of the dam and foundation for the homogeneous model. To determine the interior stresses in the dam, stresses obtained along this section were taken as the boundary stresses and eqns. (3) to (5) were solved.

4.2. *Determination of interface stresses*

Interface stresses[9] can be determined directly using the continuity conditions and photoelastic data. The continuity conditions along the interface can be written as [Fig. 1]:

$$(\sigma_y)_1 = (\sigma_y)_2; \quad (\varepsilon_x)_1 = (\varepsilon_x)_2; \quad (\tau_{xy})_1 = (\tau_{xy})_2. \tag{14}$$

From the photoelastic data, the difference in normal stresses can be determined as

$$(\sigma_y)_1 - (\sigma_x)_1 = N_1(F_\sigma)_1 \cos 2\theta_1 \tag{15}$$

$$(\sigma_y)_2 - (\sigma_x)_2 = N_2(F_\sigma)_2 \cos 2\theta_2$$

where subscripts 1 and 2 stand for body 1 and 2, and $F_\sigma = f_\sigma/t$.

Using eqn. (14), the stress-strain relations in two-dimensions and eqn. (15), σ_y can be determined as

$$\sigma_y = \frac{-(E_1/E_2) N_2(F_\sigma)_2 \cos 2\theta_2 + N_1(F_\sigma)_1 \cos 2\theta_1}{(1 - v_1)/(E_1/E_2)(v_2 - 1)} \tag{16}$$

Using the above equation, σ_y can be computed along the interface. After determining σ_y, $(\sigma_x)_1$ and $(\sigma_x)_2$ can be determined using eqn. (15).

The shear stress τ_{xy} along the interface can be obtained as

$$\tau_{xy} = (\tau_{xy})_1 = (\tau_{xy})_2 = \frac{N_1(F_\sigma)_1}{2} \sin 2\theta_1$$

$$= \frac{N_2(F_\sigma)_2}{2} \sin 2\theta_2. \tag{17}$$

In two-dimensional problems it is assumed that in-plane loads are applied symmetrically with respect to middle plane. As no loads are applied on the faces of the

model and as the thickness of the model is small when compared with other dimensions, the transverse normal stress is ignored. This assumption is not valid if out of plane displacement is restrained particularly when one material is bonded to another relatively rigid material. This effect is referred to as pinching effect by some investigators[13] and can introduce significant errors particularly in the measured photo-elastic data. However, it is possible to assess the pinching effect in two-dimensional composite model by independently computing the shear stress (τ_{sy}) from the photoelastic data for the two bodies along the interface. If the pinching effect is negligible, then such a computation will give along the interface the same shear stress distribution. In the particular problem considered here, the pinching effect was negligible.

5. Results and discussion

Stresses in both the homogeneous and composite models, with and without opening, were frozen using the stress freezing procedure described earlier. To verify whether any stresses would develop in the composite model during stress freezing procedure due to difference in coefficient of thermal expansion of the two materials, a dummy composite specimen was used and it was subjected to the same temperature cycle used for freezing the stresses inside the loaded model. Later when the dummy model was observed in the polariscope, it was found that the residual stresses were negligible.

The boundary fringe orders were then measured both for homogeneous and composite models (with and without opening) using Tardy's method. For composite models, the interface stresses were determined using the procedure described earlier. For homogeneous model, the stresses along the junction of the dam and foundation were determined using eqn. (12). From the measured/computed boundary stresses, the interior stresses were determined using eqns. (6) to (8). The grid spacing selected for solving the finite difference equations is shown in Fig. 4. A typical dark field isochromatic pattern for a dam model with the opening at the junction of the foundation and dam is shown in Fig. 5.

The normal and shear stresses obtained from photo-elasticity along different sections are shown in Figs. 6–8 both for homogeneous and composite cases. In these figures, the stresses obtained along different sections using the method of Creager et al[1] are also included for comparison. The distribution of normal and shear stresses in homogeneous and composite models with openings are given in Figs. 9–17. The distribution of tangential stress along the boundary of the opening is shown in Figs. 18–20. In this the distribution of tangential stress computed from: (i) theoretical stress distribution obtained from the method of Creager et al, at the centre of the hole neglecting the opening and taking these stressest he tangential stress along the hole boundary was determined using stress coefficients given by Philips and Zangar[14], (ii) using the stress distribution obtained from photoelasticity, for a model without opening at the centre of the hole and the stress coefficients of Philips and Zangar, are also included for comparison.

$n = 0.11\,b \quad (0.11\,h)$
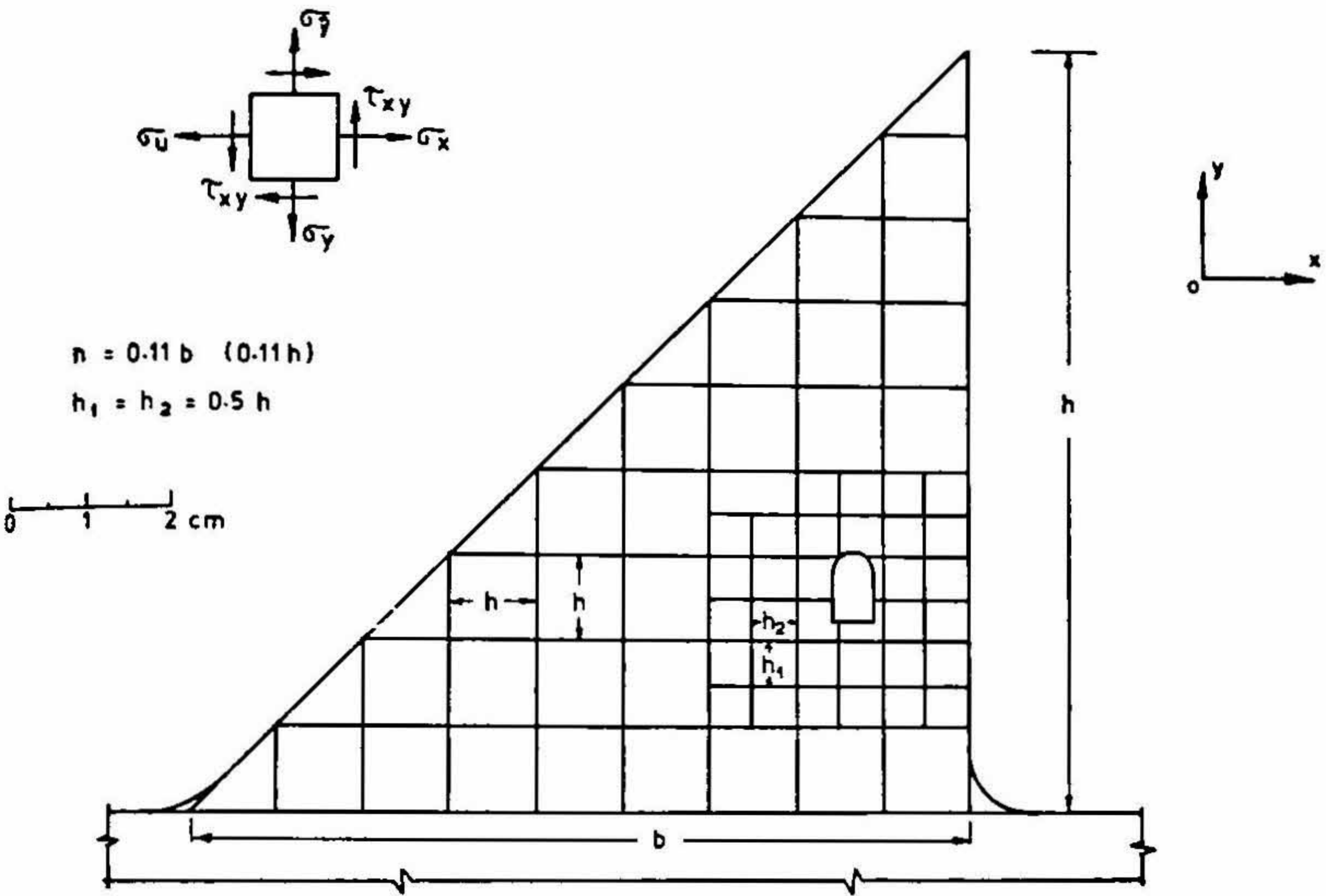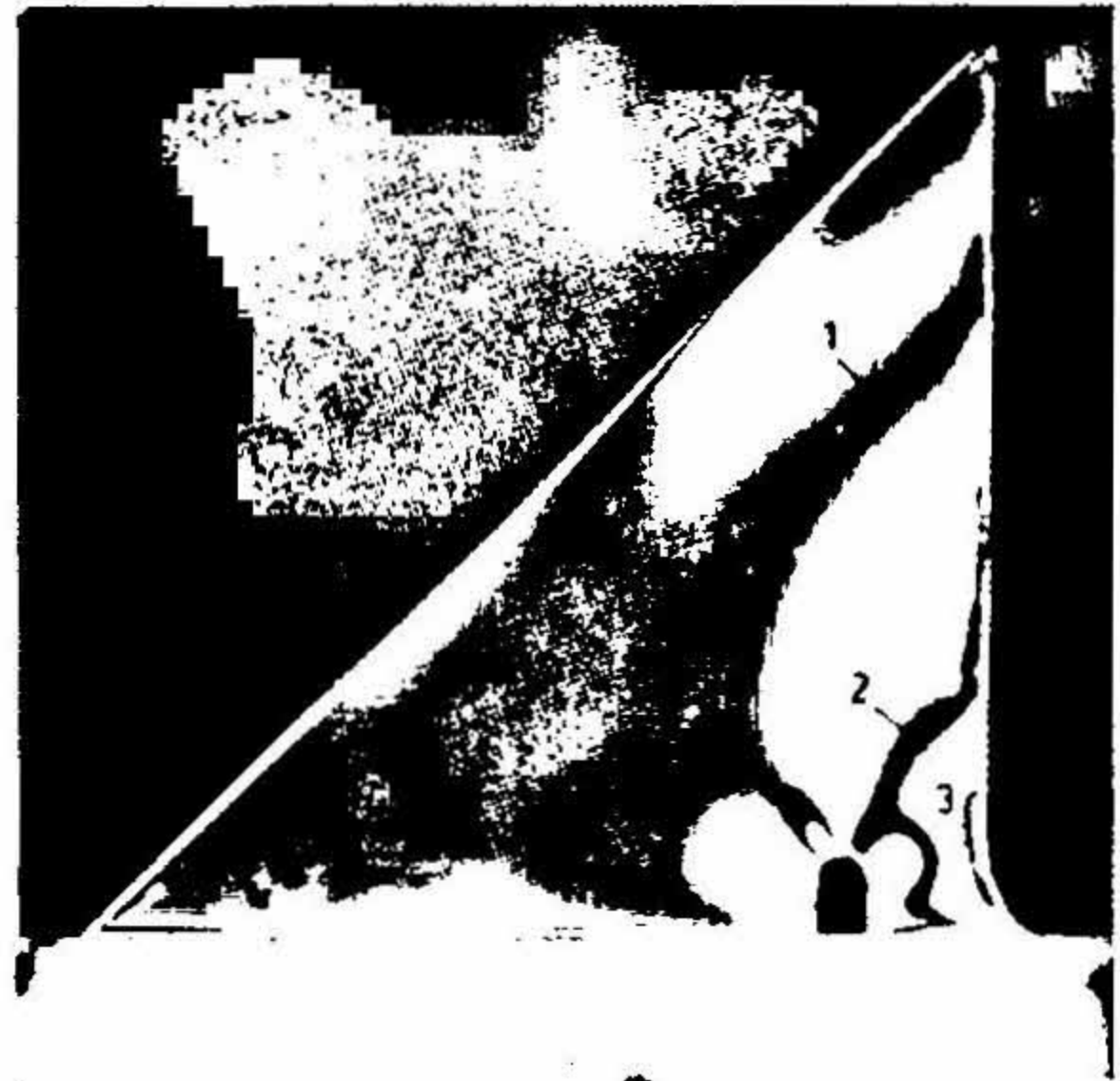
$h_1 = h_2 = 0.5\,h$

FIG. 4. Grid used for analysis.

(a) Homogeneous Case (b) Composite Case

FIG. 5. Dark field isochromatic pattern for a dam model with an opening at the junction of the dam and foundation.
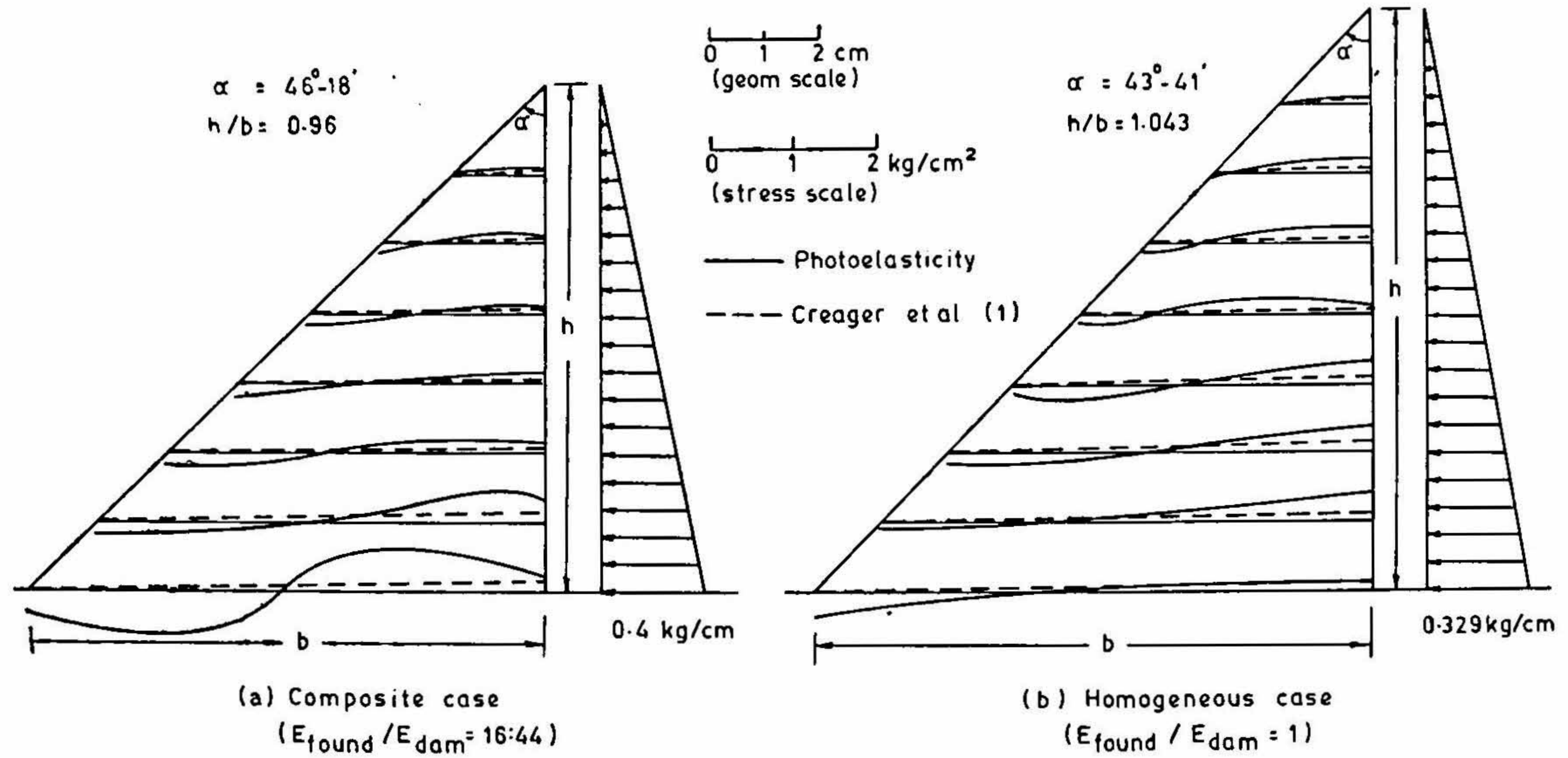
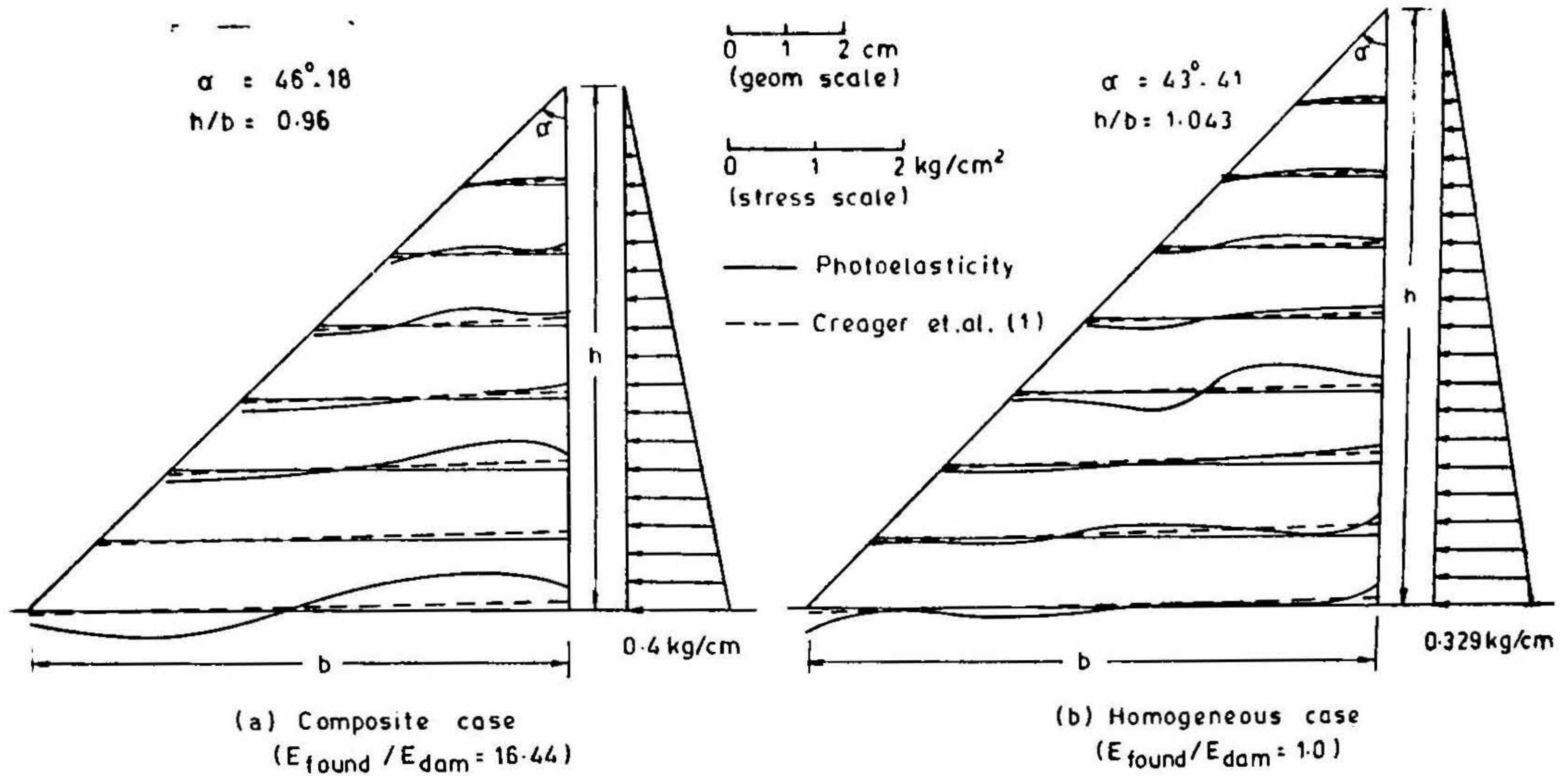FIG. 6. Distribution of vertical stress (σ_y) at different horizontal sections for a dam model.

$\alpha = 46°.18$
$h/b = 0.96$

0 1 2 cm
(geom scale)

0 1 2 kg/cm²
(stress scale)

——— Photoelasticity
- - - Creager et.al. (1)

$\alpha = 43°.41$
$h/b = 1.043$

0.4 kg/cm

0.329 kg/cm

(a) Composite case
$(E_{found}/E_{dam} = 16.44)$

(b) Homogeneous case
$(E_{found}/E_{dam} = 1.0)$

FIG. 7. Distribution of horizontal stress (σ_g) at different horizontal sections for a dam model.
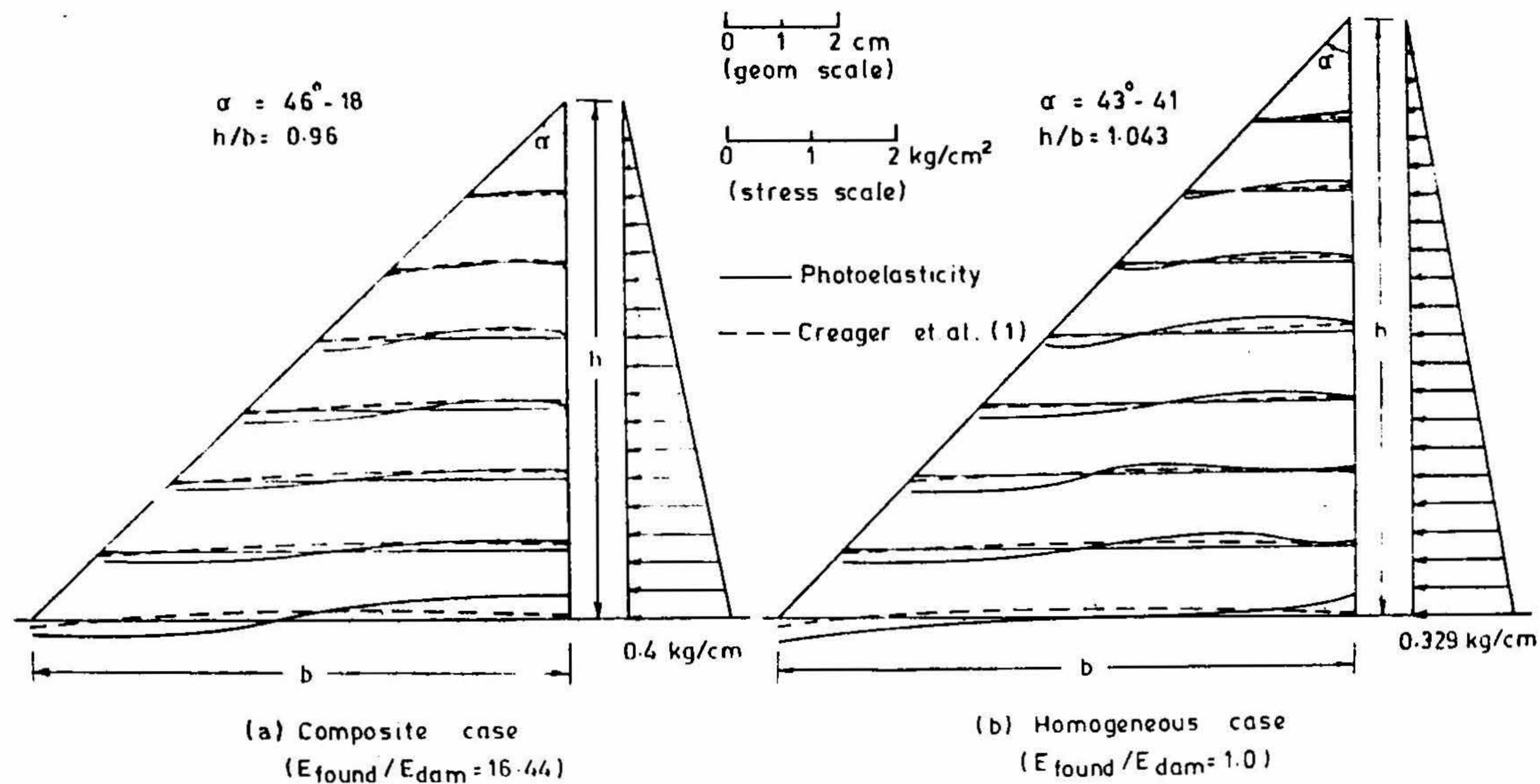
FIG. 8. Distribution of shear stress (τ_{xy}) at different horizontal sections for a dam model.
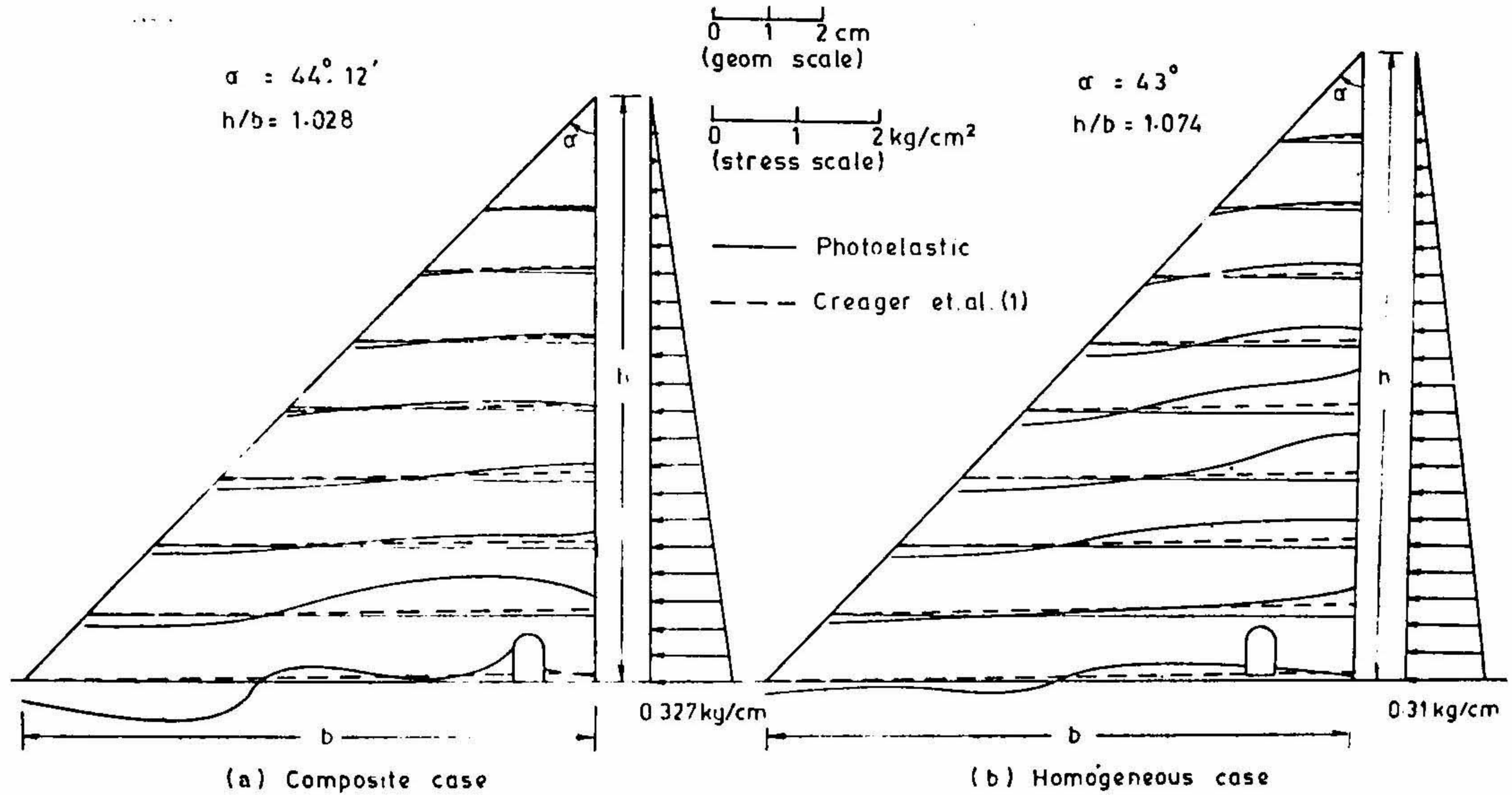
FIG. 9. Distribution of vertical stress (σ_y) at different horizontal sections for a dam model with opening at interface.
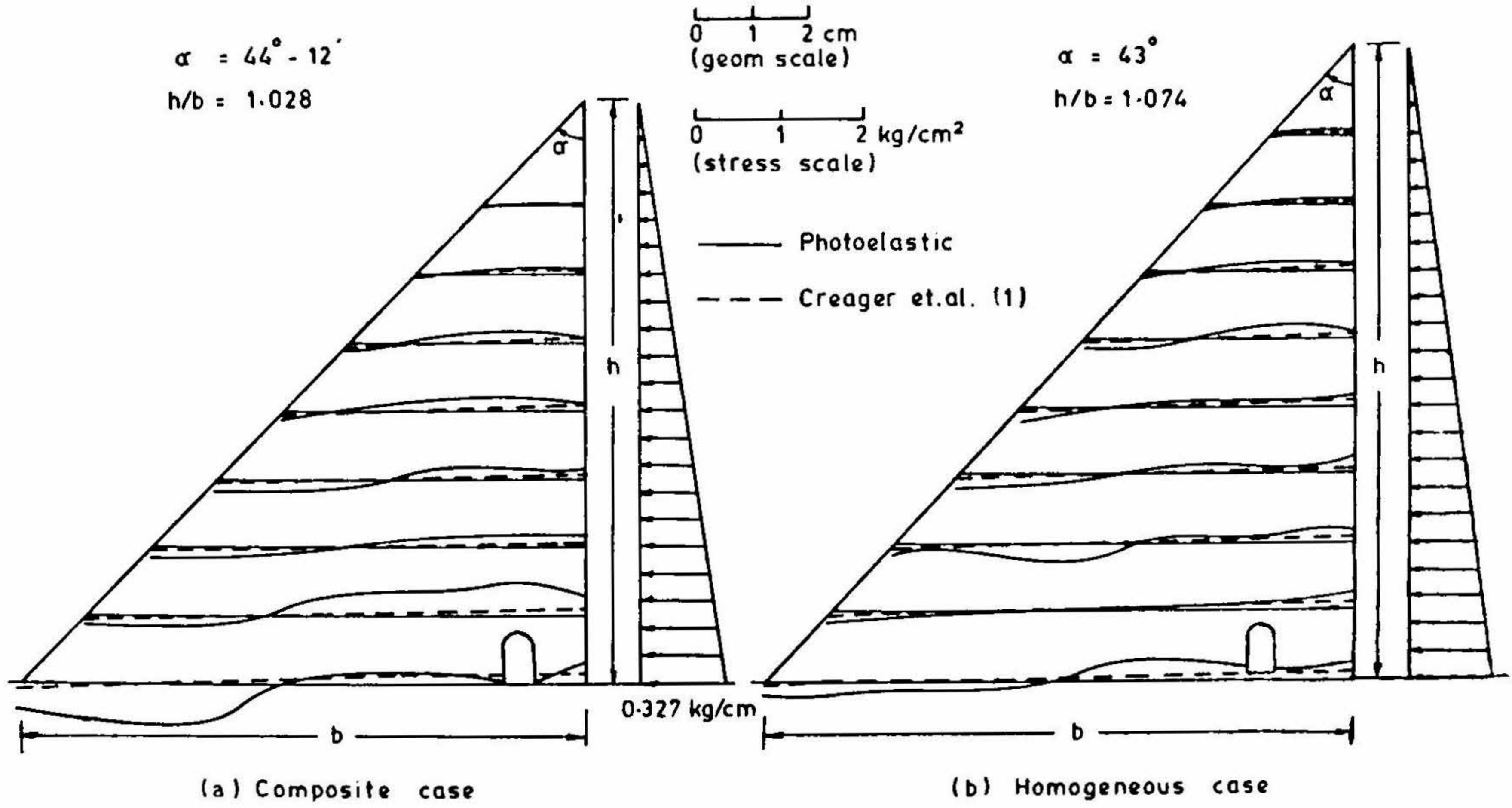
FIG. 10. Distribution of horizontal stress (σ_s) at different horizontal sections for a dam model with opening at interface.
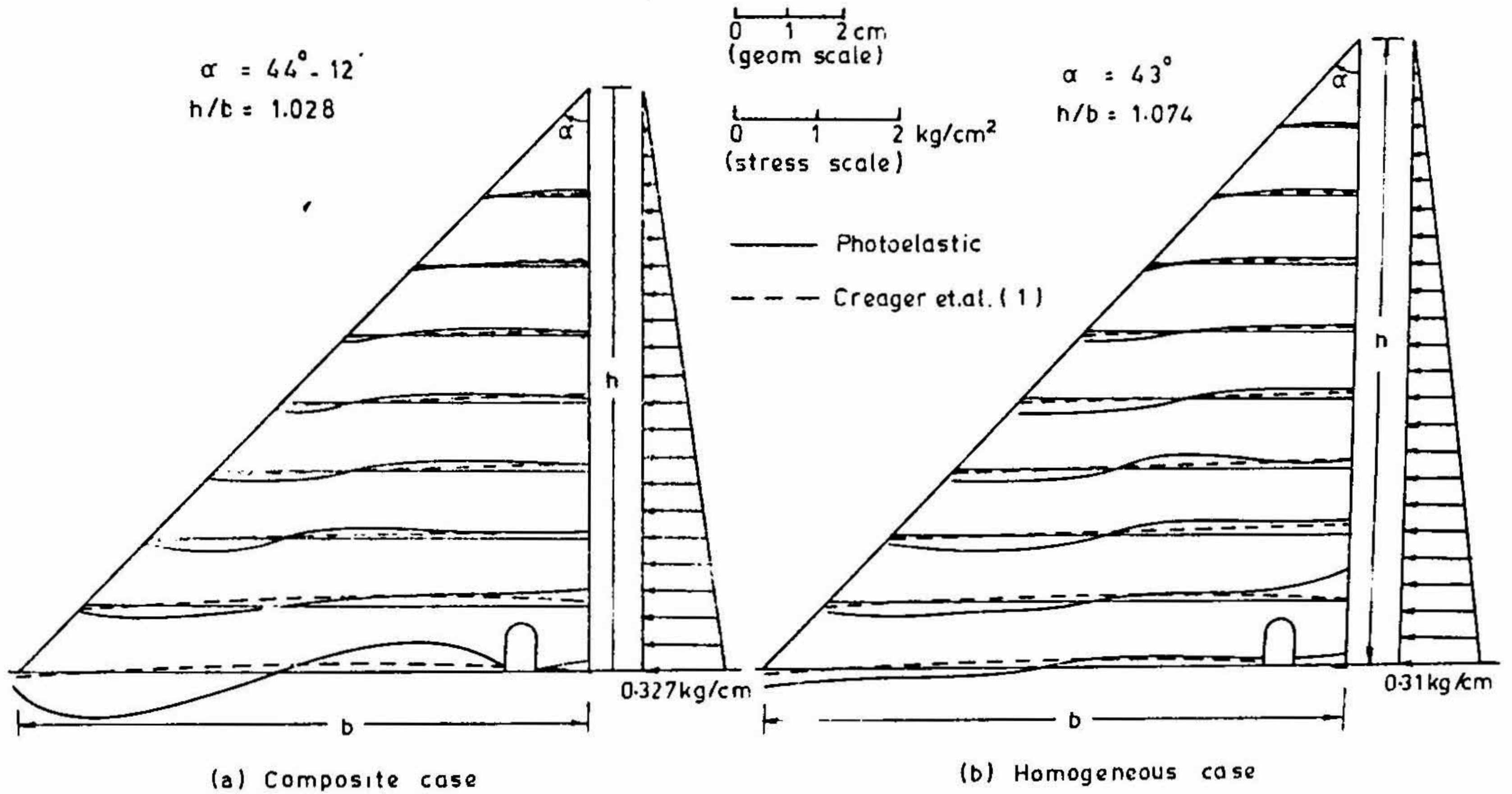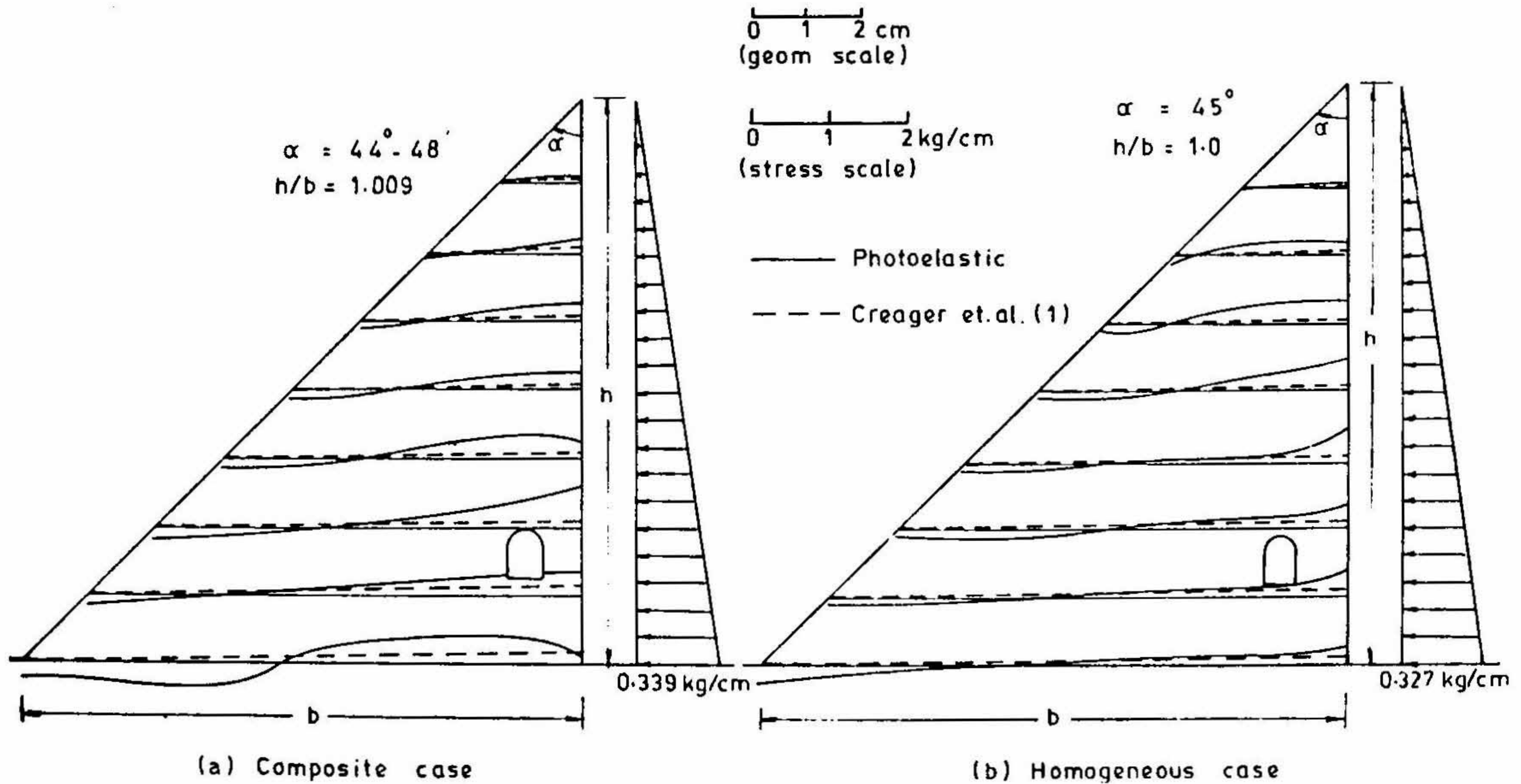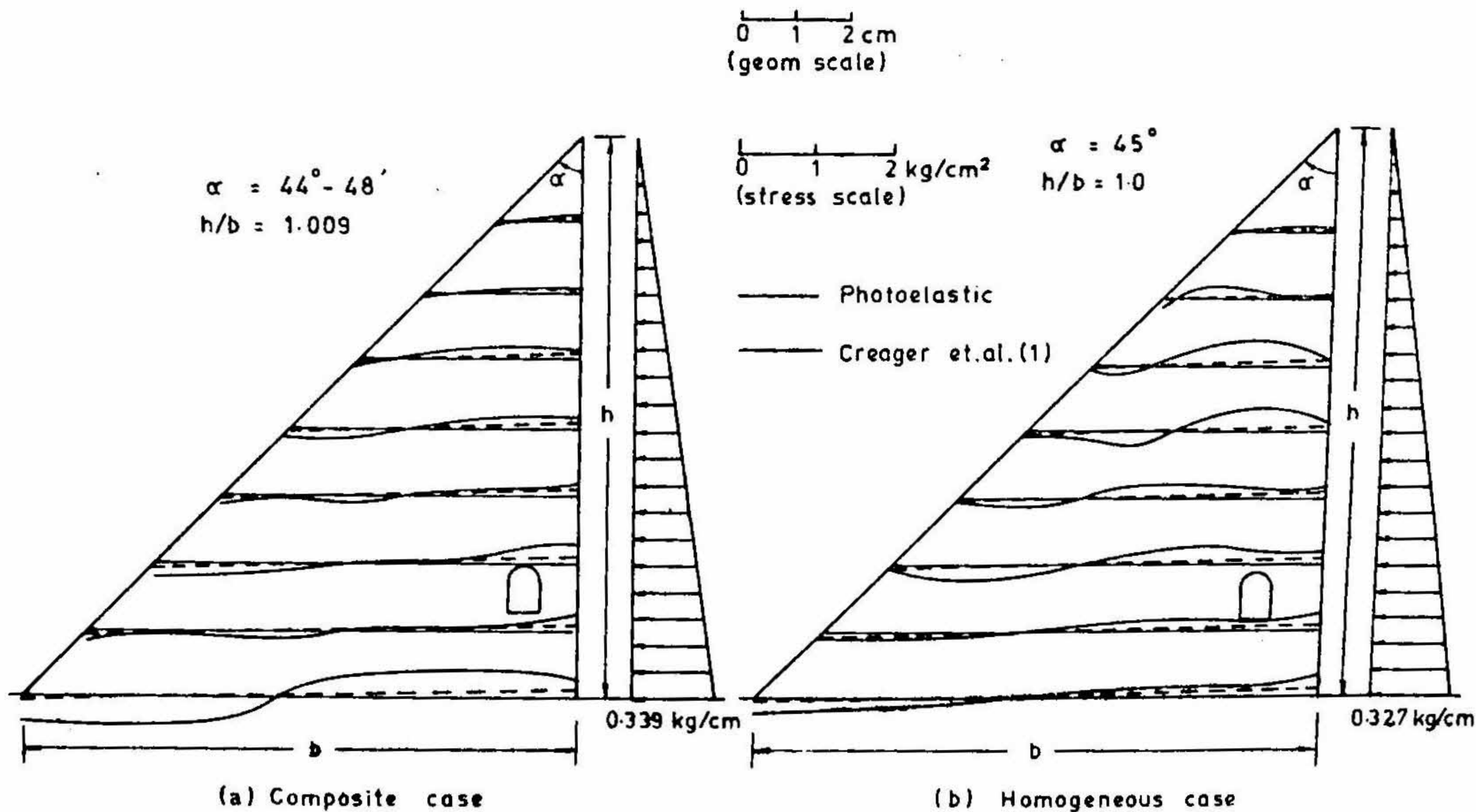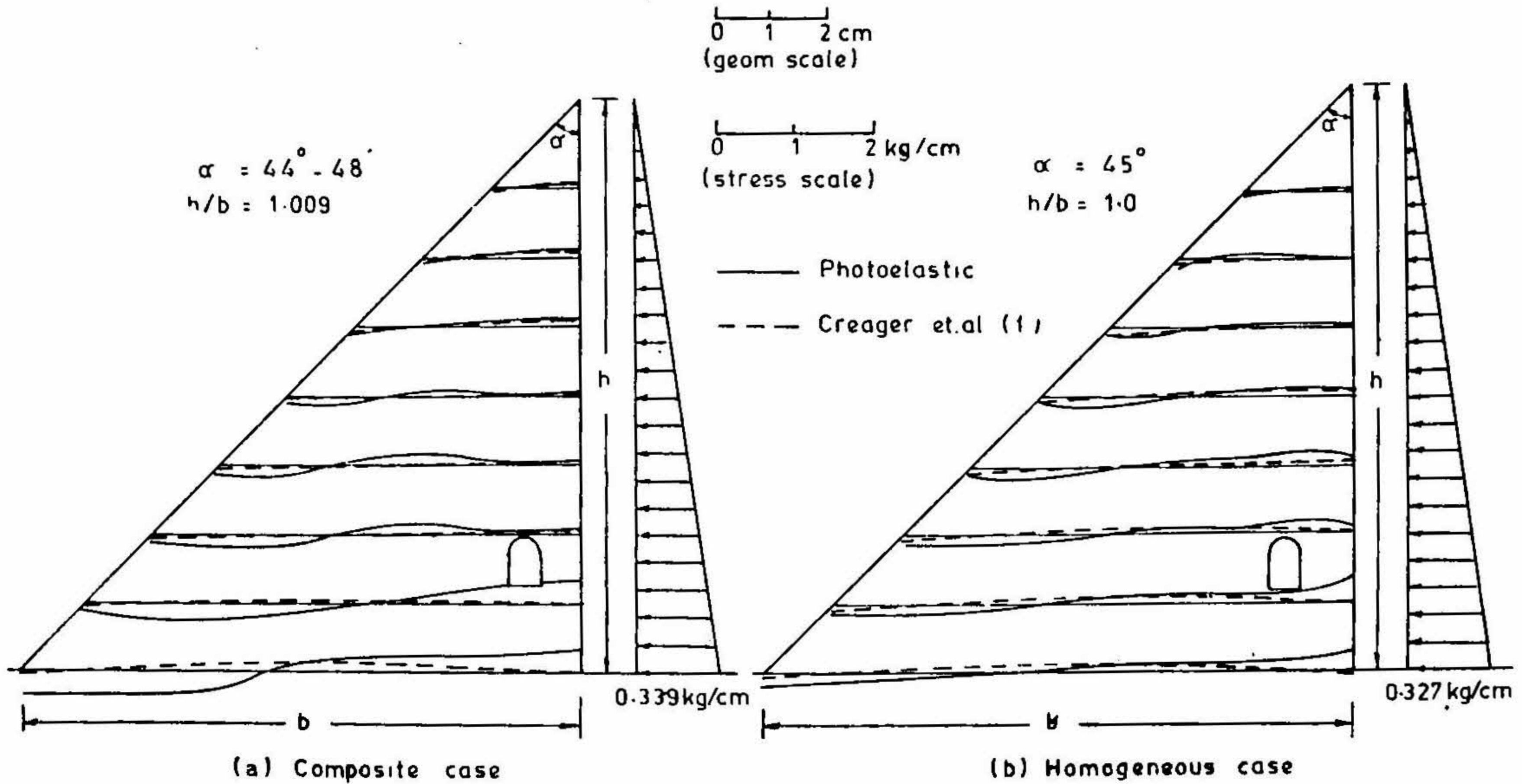
FIG. 11. Distribution of shear stress (τ_{xy}) at different horizontal sections for a dam model with opening at interface.

FIG. 12. Distribution of vertical stress (σ_y) at different horizontal sections for a dam model with opening at $1/5\,h$.

FIG. 13. Distribution of horizontal stress (σ_s) at different horizontal sections for a dam model with opening at 1/5 h.

FIG. 14. Distribution of shear stress (τ_{xy}) at different horizontal sections for a dam with model opening at 1/5 h.
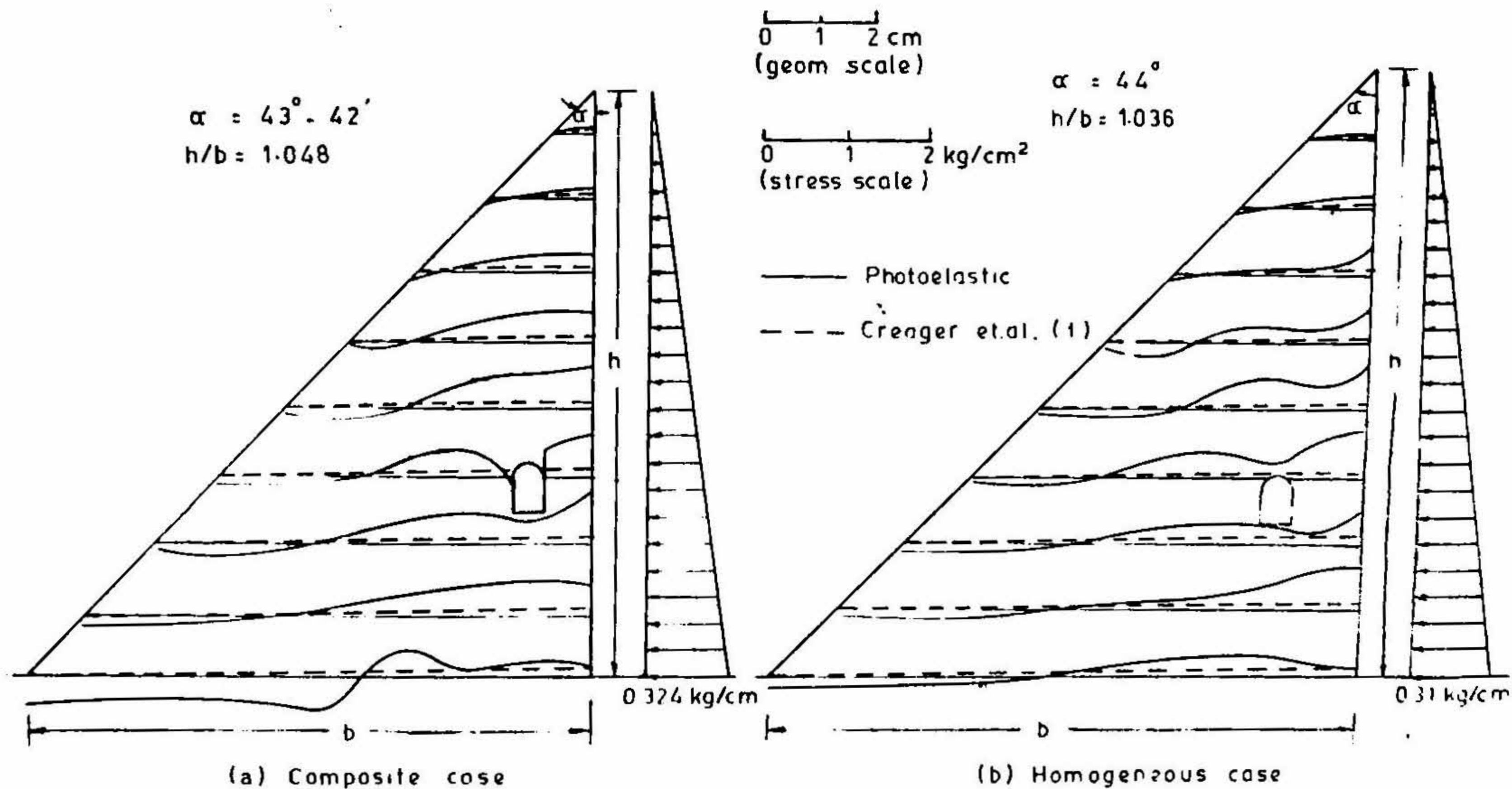
$\alpha = 43°. 42'$
$h/b = 1.048$

$\alpha = 44°$
$h/b = 1.036$

0 1 2 cm
(geom scale)

0 1 2 kg/cm²
(stress scale)

——— Photoelastic
— — — Creager et.al. (1)

0 324 kg/cm

0 31 kg/cm

b

b

(a) Composite case

(b) Homogeneous case
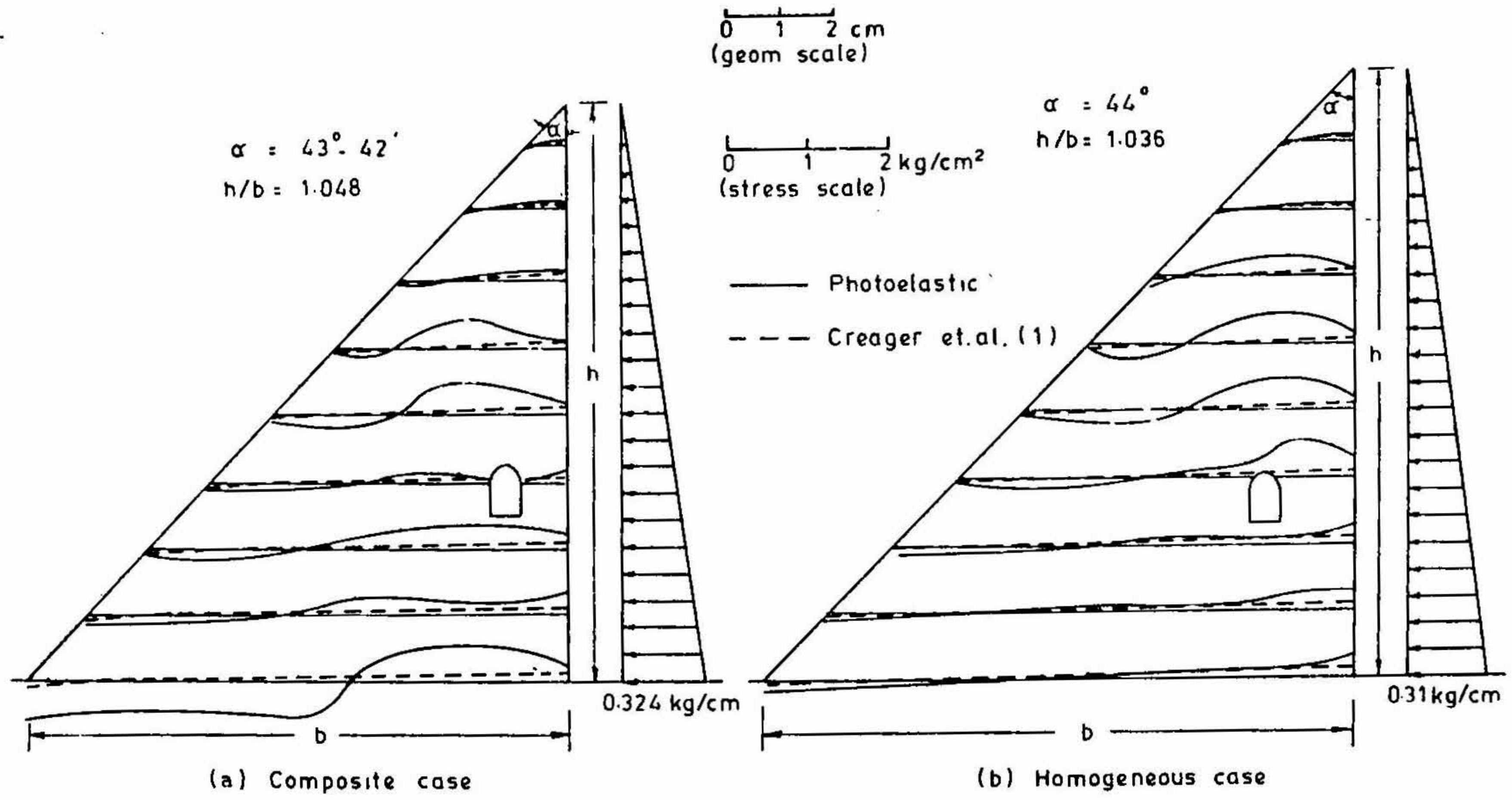
FIG. 15. Distribution of vertical stress (σ_y) at different horizontal sections for a dam model opening at 1/3 h.

Fig. 16. Distribution of horizontal stress (σ_s) at different horizontal sections for a dam model with opening at $1/3$ h.
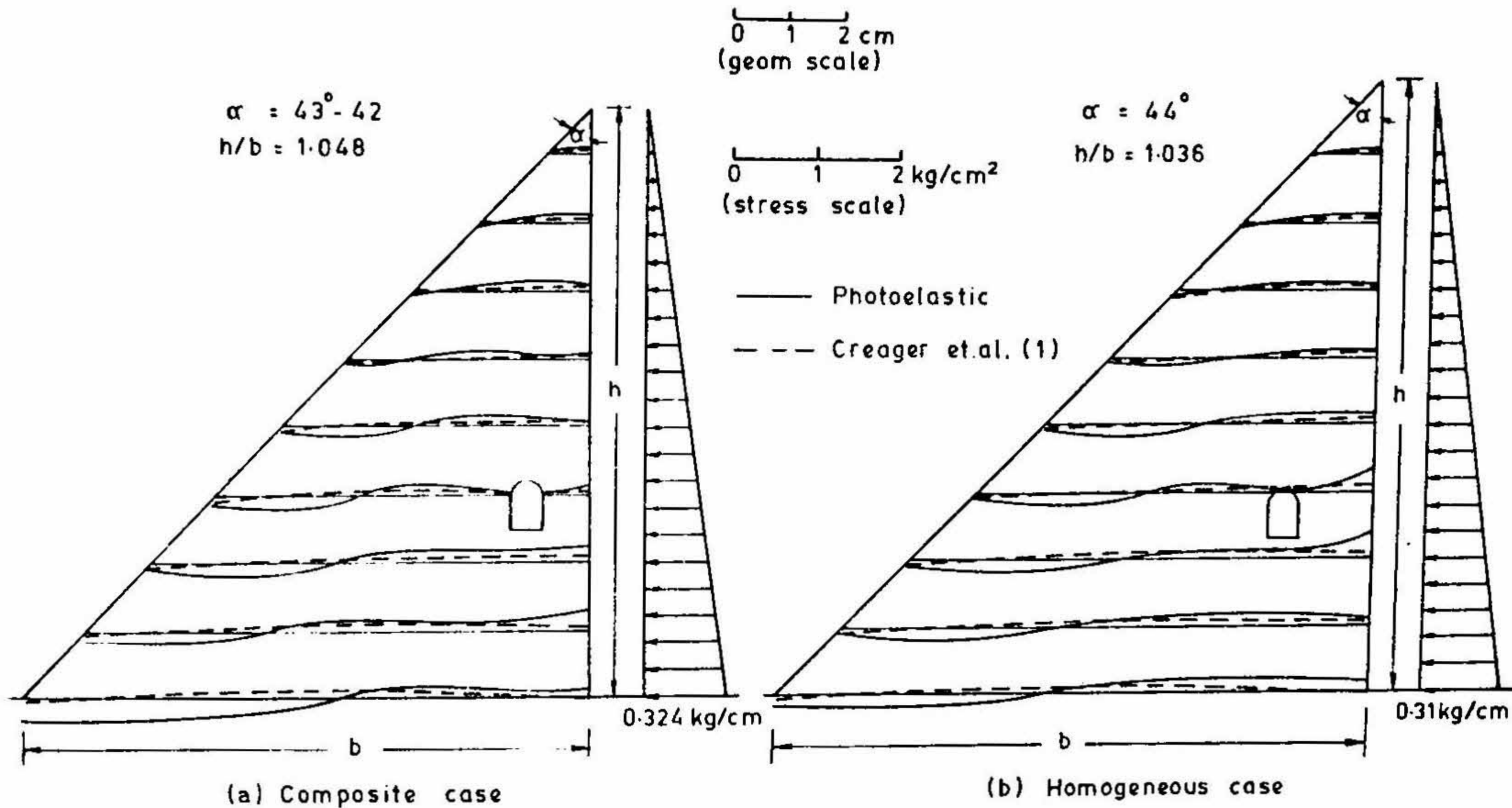
$\alpha = 43° \cdot 42$
$h/b = 1.048$

0 1 2 cm
(geom scale)

0 1 2 kg/cm²
(stress scale)

——— Photoelastic
— — — Creager et.al. (1)

$\alpha = 44°$
$h/b = 1.036$

0.324 kg/cm

0.31kg/cm

b

b

(a) Composite case

(b) Homogeneous case

FIG. 17. Distribution of shear stress (τ_{xy}) at different horizontal sections for a dam model with opening at 1/3 h.
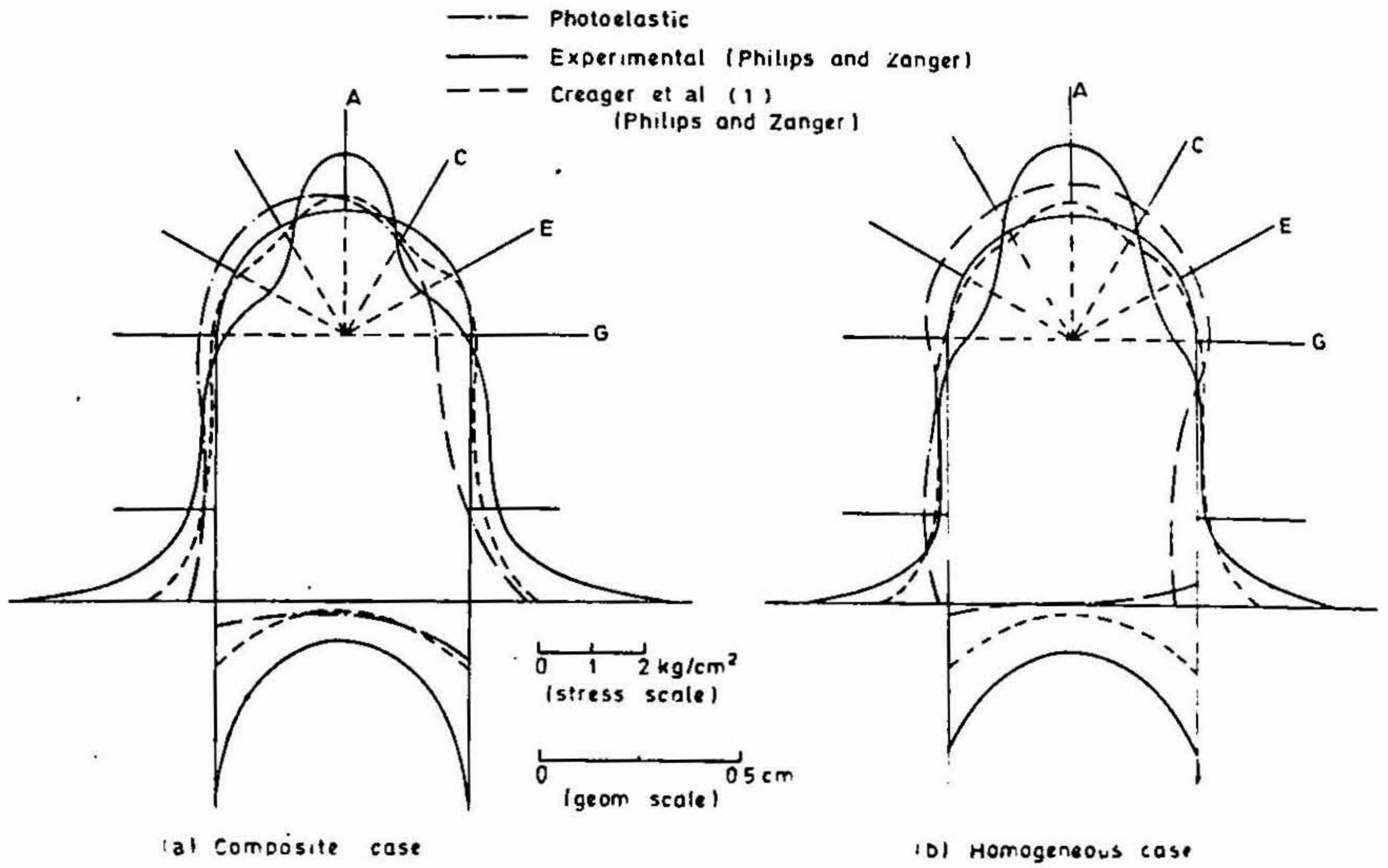
FIG. 18. Tangential stress distribution around the gallery with hole position at junction of dam and foundation level.
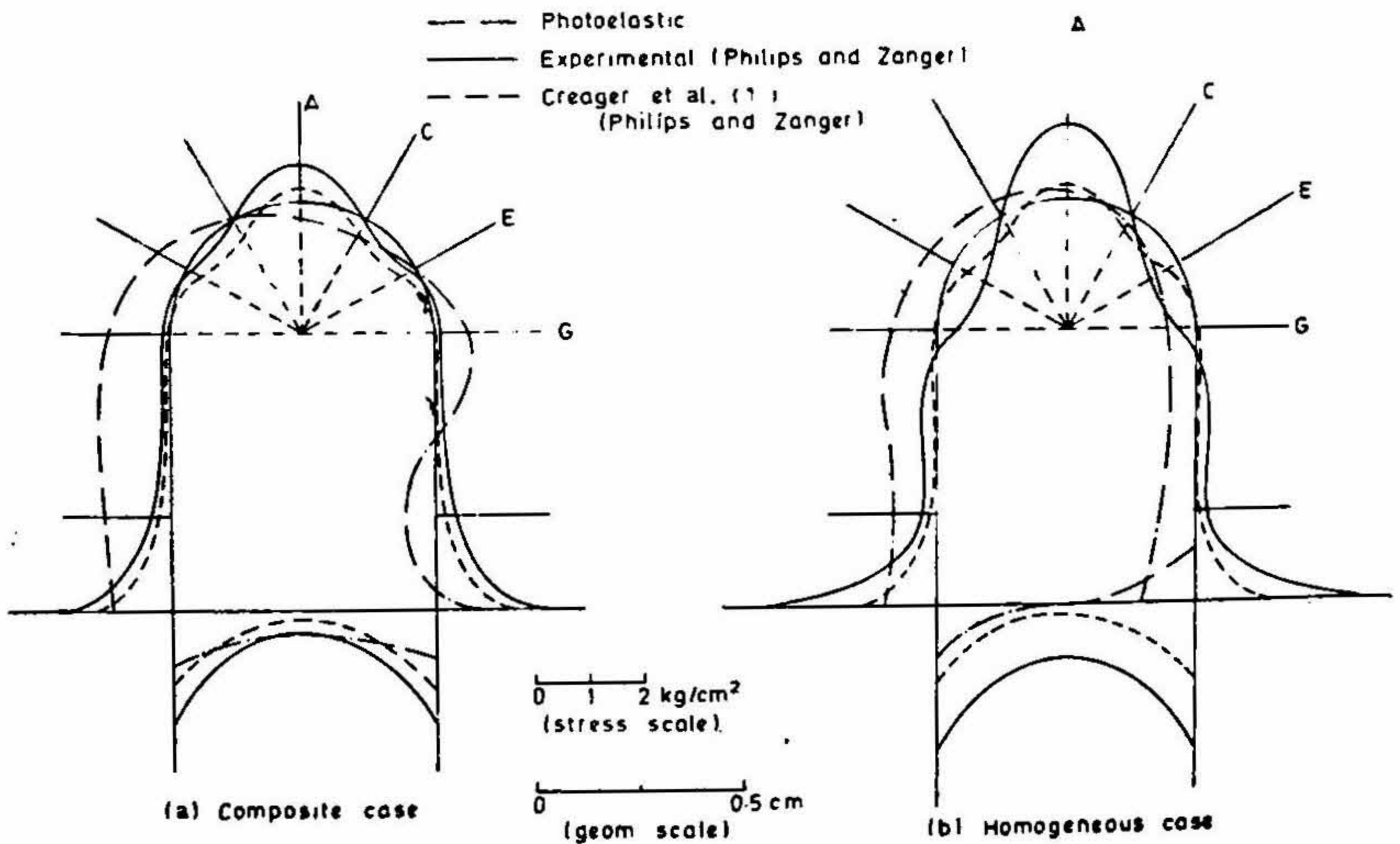

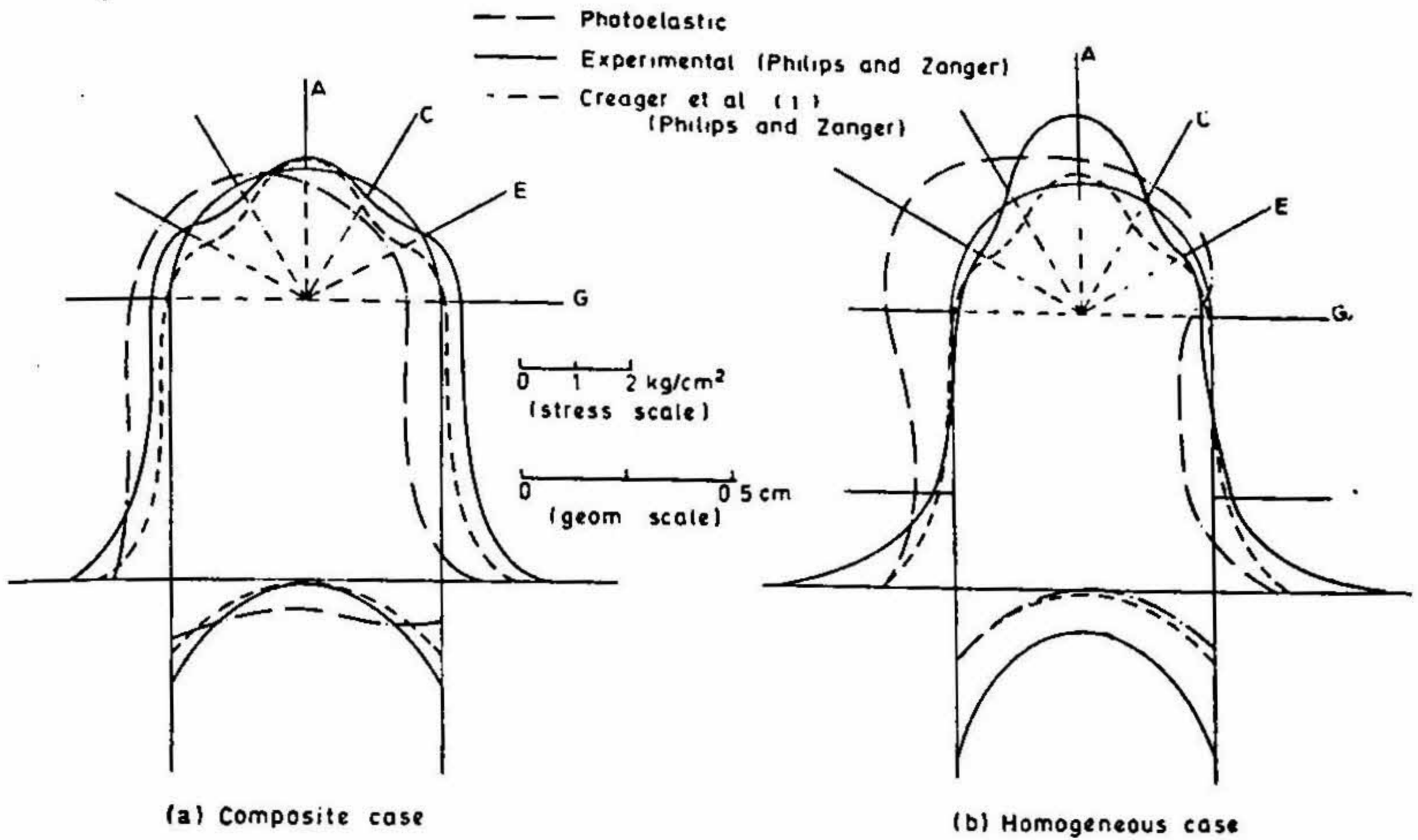FIG. 19. Tangential stress distribution around the gallery with hole position at 1/5 h from the foundation level.

FIG. 20. Tangential stress distribution around the gallery with hole position at 1/3 h from the foundation level.

The following observations can be made from Figs. 6 to 17 :

(i) The vertical stress distribution is nonlinear both for the homogeneous and composite cases at the interface and in the bottom two third portions of the dam. However, the nonlinearity is more in the case of composite dam.

(ii) The vertical stress is tensile at the heel of the dam and the magnitude of the stress is higher for the composite compared to homogeneous case.

(iii) The magnitude and distribution of vertical, horizontal and shear stresses obtained along different sections from experiment do not agree with those predicted by Creager et al method.

(iv) The presence of an opening distorts the stress distribution only locally. However, the region of distortion is higher for the composite case when compared with the homogeneous case.

It may be seen from Figs. 18 to 20, that the tangential stress distribution obtained on the boundary of the opening using Creager et al and Phillips and Zangar stress coefficients is much smaller than that obtained from experiment. On the other hand,

if the stress distribution at the centre of the hole could be obtained accurately taking into account the foundation elasticity effect, then the tangential stress distribution due to these stresses around the opening can be determined using the stress coefficients given by Phillips and Zangar. This method gives the maximum value of the tangential stress higher than that given by the experiment and hence could be safely used for the design.

Acknowledgement

References

1. CREAGER, W. P., JUSTIN, J. D. AND HINDS, J.

   Engineering for Dams, 2, John Wiley, 1945.

2. CHANDRASHEKHARA, K.

   Stress analysis in gravity dams, *J. Sci. Ind. Res.*, 1961, 20A (7), 377.

3. RYDZEWSKI, J. R.

   Stress distribution in gravity dams, *Water Power*, 1960, 12, 239.

4. ZIENKIEWICZ, O. C. AND GERSTNER, R. W.

   Foundation elasticity effects in gravity dams, *Proc. Instn. Civ. Engrs. (London)*, 1961, 19, 209.

5. VARSHENEY, R. S.

   Dams on rocks of varying elasticity, *Int. J. Rock Mech. Min. Sci.*, 1974, 11 (1), 1.

6. VARSHENEY, R. S.

   Contact stresses in gravity dams, *Indian Concr. J.* 1974, 48 (11), 355–363.

7. CHANDRASHEKHARA, K.

   Two- and three-dimensional photo-elastic analysis of composite media, Final Report to the University Grants Commission, New Delhi, Department of Civil Engineering, Indian Institute of Science, Bangalore.

8. DURELLI, A. J. AND RILEY, W. E.

   Introuction to photomechanics, Prentice Hall, 1965.

9. CHANDRASHEKHARA, K. AND ABRAHAM JACOB, K.

   Two-dimensional analysis of composite bodies, *Prog. Expl. Mech.*, Durelli Anniversary volume, Catholic Univ. of America, Washington D.C., 1975, p. 131.

10. CHANDRASHEKHARA, K. AND ABRAHAM JACOB, K.

    An experimental numerical hybrid technique for two-dimensional stress analysis, *Strain*, 1977, 13 (1), 25.

11. DURELLI, A. J. AND FERRER, L.

    New methods to determine elastic constants, *Mater. Res. Stand.*, 1963, 3 (12), 988.

12. CHANDRASHEKHARA, K. AND ABRAHAM JACOB, K.

    A method for separation of stresses in two- and three-dimensional photoelasticity, *J. Indian Inst. Sci.*, 1976, 58 (8), 331.

13. DURELLI, A. J. AND PARKS, V. J.

    Experimental stress analysis of loaded boundaries in two-dimensional second boundary value problems, *Expl. Mech.*, 1967, 7 (9), 381.

14. PHILLIPS, H. B. ZANGER, C. N.

    Stress around gallery determined by the photoelastic interferometer, Engineering Monograph, No. 12, U.S. Dept. of Interior Bureau of Reclamation, Apr. 1952.